Anaerobic and aerobic biodegradation of soil-extracted dissolved organic matter from the water-level-fluctuation zone of the Three Gorges Reservoir region, China

Jiang Liu [a,b], Jian Liang [a,c], Andrea G. Bravo [d], Shiqiang Wei [a], Caiyun Yang [e], Dingyong Wang [a], Tao Jiang [a,f,*]

[a] Interdisciplinary Research Centre for Agriculture Green Development in Yangtze River Basin, College of Resources and Environment, Southwest University, Chongqing 400716, China
[b] State Key Laboratory of Environmental Geochemistry, Institute of Geochemistry, Chinese Academy of Sciences, Guiyang 550002, China
[c] College of Chemistry and Environmental Engineering, Baise University, Guangxi 533000, China
[d] Department of Environmental Chemistry, Institute of Environmental Assessment and Water Research (IDAEA), Spanish National Research Council (CSIC), Barcelona, Spain
[e] Research Center of Bioenergy and Bioremediation, College of Resources and Environment, Southwest University, Chongqing 400716, China
[f] Department of Forest Ecology and Management, Swedish University of Agricultural Sciences, Umeå SE-90183, Sweden

HIGHLIGHTS

- Anaerobic DOM biodegradation is a crucial process in the WLFZ beyond the expected.
- Soil DOM biodegradation resulted in enrichment of recalcitrant component.
- SUVA$_{254}$ and BIX could track the DOM biodegradation in anaerobic conditions.
- DOM biodegradation potential in the WLFZ of the TGR region was predicted.

GRAPHICAL ABSTRACT
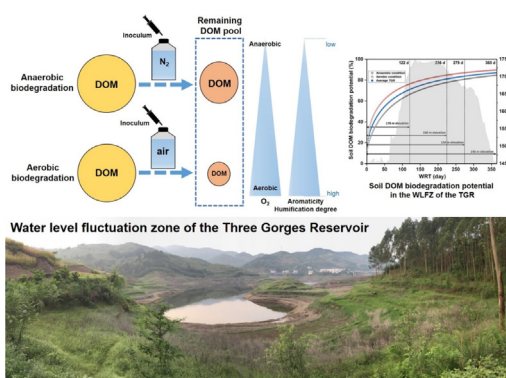
ARTICLE INFO

ABSTRACT

The biodegradation of dissolved organic matter (DOM) in natural environments is determined by its molecular composition and reactivity. Redox oscillations are common in the water-level-fluctuation zone (WLFZ) of the Three Gorges Reservoir (TGR). As a consequence, the soil DOM released is degraded under both anaerobic and aerobic conditions. The DOM compounds available for degradation under contrasting redox conditions and the resulting DOM composition still need to be elucidated. By combining laboratory experiments with an in-depth characterization of DOM optical properties, we show that different pathways controlled the depletion and enrichment of the DOM optical components under different oxygen regimes. In particular, 28-day dark biodegradation assays showed that up to $39.5 \pm 4\%$ DOM was degraded under anaerobic conditions, while $55.5 \pm 6\%$ DOM was biodegraded under aerobic conditions. Aerobic biodegradation resulted in a higher aromaticity and degree of humification of the DOM compared to anaerobic degradation. The specific UV absorbance at a wavelength of 254 (SUVA$_{254}$) and biological index (BIX) could be used to track DOM biodegradation under anaerobic conditions. Under aerobic conditions, the SUVA$_{254}$, BIX and concentration of coloured DOM (CDOM, reflected by a (355)) could track DOM biodegradation, and significant amounts of CDOM could be aerobically biodegraded.

© 2020 Elsevier B.V. All rights reserved.

---

* Corresponding author at: College of Resources and Environment, Southwest University, 2 Tiansheng Road, Beibei, Chongqing 400715, China.
E-mail address: tower@swu.edu.cn (T. Jiang).

1. Introduction

As an essential component of soil organic matter, soil dissolved organic matter (DOM) is the most active and mobile organic matter (OM) pool that links terrestrial and aquatic systems (Jansen et al., 2014; Solomon et al., 2015). Dissolved organic matter not only influences global carbon cycling (Evans et al., 2017; Cory and Kling, 2018) but also has a significant influence on the biogeochemical process of nutrients (Mao et al., 2017; Fasching et al., 2020) and environmental contaminants including trace metals and organic contaminants (Hur et al., 2011; Aiken et al., 2011). The most recognized biogeochemical characteristics responsible for DOM processing include photodegradation and biodegradation (Moran et al., 2000; Obernosterer and Benner, 2004; Stedmon and Markager, 2005; Hansen et al., 2016; Cory and Kling, 2018), redox abilities (Gao et al., 2019; Jiang et al., 2020a, 2020b), binding capacities with other elements, such as heavy metals (Jiang et al., 2015), and adsorption by minerals (Lee et al., 2018). In particular, DOM biodegradation has a key role, as it results in CO_2 and CH_4 emissions, which are directly linked with different global climate change scenarios (Berggren et al., 2010; Gao et al., 2019; Grasset et al., 2018).

The biodegradation of DOM occurs either in terrestrial or aquatic environments in both euphotic and/or dark zones. Although light-induced changes in DOM seem to trigger DOM biodegradation (Moran et al., 2000; Stedmon and Markager, 2005), most of the photochemistry of DOM can only be observed in the uppermost layer of water columns (*i.e.*, euphotic zone) (Kothawala et al., 2012; Sulzberger and Arey, 2016). Actually, in freshwater systems, 1.2 Pg of CO_2 originating from DOM is transported into the atmosphere annually, and most of the CO_2 is metabolized by heterotrophic microorganisms (Tranvik et al., 2009; Sleighter et al., 2014). In soil, microbial degradation can account for 10 to 44% of DOM loss, and this value might even increase to approximately 75% in litter (Hongve et al., 2000; Kalbitz et al., 2003a). Additionally, DOM biodegradation has further environmental implications for contaminant fate, for example, mercury (Hg) (Jiang et al., 2018a; Schartup et al., 2013; Bravo et al., 2017; Herrero Ortega et al., 2017). Recent studies (Schartup et al., 2013; Bravo et al., 2017; Herrero Ortega et al., 2017; Noh et al., 2018; Jiang et al., 2018a) demonstrated that differences in the composition of DOM may largely explain the variability in the formation of neurotoxic methylmercury. Hence, the quantification and characterization of DOM biodegradation processes are required for the understanding of the global carbon cycle and the fate of pollutants.

DOM biodegradation is controlled by many factors, including intrinsic DOM composition, geo-physico-chemical properties (*e.g.*, salinity, temperature, pH, and oxygen concentration) and microbial community structure (Marschner and Kalbitz, 2003). Among all of the influencing factors, the DOM chemical diversity (*i.e.*, DOM compositional characteristics) seems to be a primary controlling factor of DOM microbial utilization (Shen and Benner, 2020). Additionally, the molecular O_2 concentration is key to determining the microbial community structure and metabolic pathways involved in DOM processing. Lower DOM biodegradation has been reported in the absence of O_2, which has been explained by the following: (1) a lower energy yield due to the lower substrate utilization efficiency by heterotrophic bacteria and (2) the absence of attacks from oxygen species or oxygenases (Marschner and Kalbitz, 2003; Bastviken et al., 2004; Reimers et al., 2013). Studies have shown that the exposure of O_2 stimulates microbial activity to degrade refractory OM pools, especially for communities that are capable of extracellular electron transfer (Burdige, 2007; Reimers et al., 2013). Although the biodegradation of DOM in different anoxic and oxic environments has been studied (Kristensen et al., 1995; Bastviken et al., 2004; Reimers et al., 2013; Grasset et al., 2018; Valle et al., 2018), the outcomes of these studies were not consistent. Notably, while there was no significant difference in OM degradation between oxic and anoxic conditions in some short-term incubation studies

(Lee, 1992; Derrien et al., 2019), other studies reported higher degradation rates under oxic conditions (Kristensen et al., 1995; Sun et al., 2002; Bastviken et al., 2004; Reimers et al., 2013). Therefore, DOM biodegradation processes in redox oscillated conditions and their contribution to the degradation of the entire DOM pool are still not fully understood. Particularly, only a few previous studies emphasized the anoxic/oxic degradation of DOM but lacked the tracking of changes in DOM properties, especially by using optical tools (Bastviken et al., 2004; Reimers et al., 2013; Grasset et al., 2018). Since optical properties (*i.e.*, absorbance and fluorescence) have been illustrated as a useful approach to assess the biodegradation processes of DOM (Wickland et al., 2007; Cory and Kaplan, 2012; Hansen et al., 2016), we extended this method to track DOM biological degradation under anaerobic and aerobic conditions.

The water level fluctuation zone (WLFZ, 306 km^2) of the Three Gorges Reservoir (TGR) region is one of the largest redox oscillated freshwater systems in the world (Bao et al., 2015). The water level is regulated at 145 m in summer and 175 m in winter for the primary purposes of flood control and electricity generation (Bao et al., 2015). Due to the frequent wetting and drying rotations, OM in riparian and upland soils is the most important terrestrial origin for DOM in adjacent aquatic systems (Jiang et al., 2017, 2018b, 2018c, 2020a). Especially, during the submerging period (usually from August to June), the DOM released from submerged soils into the water column is the most crucial pathway for terrestrial OM to reach the aquatic system. Thus, soil DOM is subjected to both oxic and anoxic conditions in water-level-fluctuation zones of TGR areas. The O_2 regimes for soil-released DOM biodegradation are heavily dependent on the elevation (*i.e.*, influenced by water level changes). The temporal and spatial variations in the DOM from waters and soils in this area have been investigated in our previous study (Jiang et al., 2018b) and others (Wang et al., 2019). However, DOM compositional changes resulting from anoxic or oxic biodegradation in this area remain unclear, which may further significantly influence the environmental implications of DOM.

In this study, we hypothesized that (1) the DOM changes caused by anaerobic and aerobic biodegradation conditions are different and (2) optical properties can be used to track the biodegradation of DOM. Thus, we conducted a series of microcosm experiments in this study. The optical properties were used to reflect the compositional changes of WLFZ soil-extracted DOM in biodegradation assays under both anaerobic and aerobic conditions. The aim of this study was two-fold: (1) to understand the biodegradation dynamics of soil-extracted DOM under different O_2 regimes and explore the changes in the DOM composition due to anaerobic and aerobic biodegradation and (2) to determine whether there are characteristic parameters of DOM that could be used to indicate its biodegradation potential under the two distinguished conditions (*i.e.*, anaerobic *vs.* aerobic).

2. Materials and methods

2.1. Soil sample collection and DOM extraction

Soil samples were collected from the water level fluctuation zone (WLFZ) of the TGR in China. To represent the four sites selected by the long-term DOM monitoring project, Zhenxi of Fulin (FL), Shibaozhai of Zhongxian (SB), Tujing of Zhongxian (TJ) and Hanfeng Lake of Kaixian (KX) (Jiang et al., 2018b) were included in this study (Fig. S1). Details of these sites were described in our previous studies (Jiang et al., 2017, 2018b). At each site, surface soils (0–10 cm) were collected from different elevations (155 m and 165 m) along the shoreline of the Yangtze River, and five samples were collected at each elevation by a zig-zag pattern. Soils collected from the same site were mixed to eliminate the differences from elevations (*e.g.*, submerging period). Visible rocks, plant residues and animals were removed from the soils. Due to the water level regulations, both re-exposed sediment (deposited

during submerging periods) and shoreline soil were included in our collected samples and defined as soil samples in this study.

Air-dried and homogenized (ground to 0.2 mm) soil samples were used to extract the DOM according to the method from Yu et al. (2012) and Jiang et al. (2017). The DOM in soil was extracted by distilled water (Milli-Q®, Millipore, USA) with a soil to water ratio (w/v) of 1:10 for 16 h in a horizontal shaker (200 rpm) under dark conditions at 25 °C. The suspension was centrifuged (4000 rpm) for 30 min and was vacuum filtered by 0.22-μm mixed cellulose acetate filters (Whatman, USA). The isolated filtrates (*e.g.*, DOM sample) were stored in the dark at 4 °C before use. The DOM samples extracted in this study have also been referred to as water soluble OM (Nierop and Buurman, 1998).

2.2. Inoculum preparation

Indigenous populations of microbial communities in soils were used as the inoculum in the degradation (Kalbitz et al., 2003a; Hansen et al., 2016). Briefly, fresh soils (*i.e.*, collected from fields with no drying treatment) from FL, SB, TJ, and KX were incubated for 7 days at 25 °C. Afterwards, indigenous microorganisms from each soil were extracted by Milli-Q water (soil/water 1:10, w/v) for 12 h with the same soil DOM extraction conditions. The obtained microorganism solutions from the four sites were left to stand for 1 h and were filtered by 20–25 μm sterile membranes to separate large organisms and particulates. Four filtered microorganism solutions (*i.e.*, FL, SB, TJ and KX) were mixed with equal volumes as the inoculum. No further microbial identifications were performed.

2.3. DOM biodegradation assay

The biodegradation of soil-extracted DOM was conducted in anaerobic and aerobic conditions at 25 °C. Mixed inoculum extracted from collected soils was used as the microorganism source in DOM biodegradation (Kalbitz et al., 2003a, 2003b). Before the biodegradation assay, DOM solutions with DOC concentrations higher than 20 mg L^{-1} were diluted to avoid the overgrowth of microorganisms (Hongve et al., 2000; Kalbitz et al., 2003b). The DOM solutions were inoculated with mixed inoculum at a ratio of 1:150 (v/v). Then, NH_4NO_3 (10 μM) and KH_2PO_4 (1 μM) were added as additional nutrients. Anaerobic treatments were incubated in 100-mL airtight serum bottles after pre-deoxygenation through high purity N_2 purging with a headspace of 20 mL of N_2. For comparison, aerobic treatments were conducted by soil-extracted DOM incubated in 100-mL amber bottles and with a headspace of 20 mL of air (Fig. S1). All bottles were precovered with aluminium foil to avoid photoreactions of the DOM. All supplies and glassware were autoclaved before use. Three replicates were set for each treatment (four soil extracted DOM solutions and two incubation conditions). The blank was non-inoculated Milli-Q® water. Biodegradation kinetic experiments were conducted over 28 days. Time-dependent sampling was conducted on 0, 1, 2, 5, 8, 12, 16, 21, and 28 d. All the collected water samples were then filtered through 0.45-μm cellulose acetate filters and kept at 4 °C (in the dark) before analysis.

2.4. Analytical measurements

The concentration of DOM, represented as dissolved organic carbon (DOC), was measured using a TOC analyser (GE InnovOx®, GE, US). The optical properties of DOM were characterized by UV–vis absorption and fluorescence spectra through Aqualog® absorption-fluorescence spectroscopy (Jobin Yvon, Horiba, Japan). Briefly, the UV–vis absorption spectra for water samples were scanned from 230 nm to 800 nm with intervals of 1 nm. Emission-excitation matrices (EEMs) of fluorescence spectra for water samples were scanned from 250 nm to 600 nm (λ_{em}, intervals of 3.18 nm) and from 230 nm to 450 nm (λ_{ex}, intervals of 5 nm) for emission and excitation spectra, respectively. More details

of the optical characterizations, including inner-filter effect correction, were described in our previous studies (Jiang et al., 2017; Liu et al., 2019b).

The UV–vis properties of DOM including the Naperian absorption coefficient at 254 nm ($a(254)$, m^{-1}), specific UV absorbance at a wavelength of 254 (SUVA$_{254}$, L mg^{-1} m^{-1}), coloured dissolved organic matter (CDOM, represented by the absorption coefficient at 355 nm, a (355), m^{-1}), spectral slopes over the ranges of 275–295 nm ($S_{275-295}$, nm^{-1}) and 350–400 nm ($S_{350-400}$, nm^{-1}), and spectral slope ratio (S_R) for $S_{275-295}$ and $S_{350-400}$ were calculated. Due to the relatively small size of the dataset and different compositions (extracted from four soils from different sampling sites) of DOM samples in this study (Fellman et al., 2009), major peaks in EEMs were identified according to the wavelength ranges defined by Coble (1996, 2007) and Coble et al. (2014) through the traditional peak-picking method. Four compounds (arbitrary units (A.U.)) including peak A ($\lambda_{ex} = 250–260$ nm, $\lambda_{em} = 380–460$ nm, humic-like compound), peak C ($\lambda_{ex} = 330–350$ nm, $\lambda_{em} = 420–480$ nm, fulvic-like compound), peak B ($\lambda_{ex} = 230$ nm, $\lambda_{em} = 300–310$ nm, protein-like compound) and peak T ($\lambda_{ex} = 230$ nm, $\lambda_{em} = 320–340$ nm, protein-like compound) were identified. Fluorescence indices including the fluorescence peak ratios ($r(A/C)$ and $r(T/C)$), fluorescence index (FI), humification index (HIX) and biological index (BIX) were calculated. More details for the calculation methods can be found in our previous studies (Jiang et al., 2017, 2020a; Liu et al., 2019b).

2.5. Biodegradation kinetics

The biodegraded DOM (final to initial DOC in %) (Eq. (1)) under both anaerobic and aerobic conditions were fitted by a two-fraction first-order kinetic model (Eq. (2)) according to the assumption that DOM was composed of two fractions (*i.e.*, labile and stable) with different degradabilities and degradation rates (Kalbitz et al., 2003a; Wickland et al., 2007; Jiang et al., 2018a). Nonlinear fitting was conducted in Origin 18.0 Software (OriginLab®, MA, USA). The adjusted R^2 was used to reflect the goodness of fit.

$$\text{Biodegraded DOM (final to initial DOC in\%)} = \frac{(DOC_0 - DOC_t)}{DOC_0} \times 100\%$$

(1)

where DOC_0 and DOC_t are the DOC concentration (mg L^{-1}) at day t and day 0 (at the beginning).

$$\text{Biodegraded DOM (final to initial DOC in\%)} = f_A \times \left(1 - e^{-k_1 \times t}\right) + f_B \times \left(1 - e^{-k_2 \times t}\right)$$

(2)

where f_A and f_B are the fractions of labile DOM and stable DOM, respectively (%) ($f_A + f_B$ was constrained to approximately 100%); k_1 and k_2 are the biodegradation rate constants of two DOM fractions (d^{-1}); and t is time (d).

The half-life (d) values of labile and stable DOM fractions were calculated through Eq. (3) according to the method from Kalbitz et al. (2003a).

$$\text{Half} - \text{life DOM}_i = \frac{\ln 2}{k_i} (i = 1 \text{ or } 2)$$

(3)

where DOM$_i$ represents DOM fractions, and k$_i$ are the biodegradation rate constants for different DOM fractions.

2.6. Prediction of the DOM biodegradation potential in the WLFZ of the TGR region

A simple prediction of the soil DOM biodegradation potential at the WLFZ in the TGR region was calculated according to Eq. (4) introduced

by Vachon et al. (2017) and the fitting results through the first-order kinetic model.

$$\text{DOM biodegradation potential} = f_L \times \frac{WRT_i \times k_L}{1 + WRT_i \times k_L} + f_S \\ \times \frac{WRT_i \times k_S}{1 + WRT_i \times k_S} \times 100\% \qquad (4)$$

where f_L and f_S are the labile and stable DOM fractions, respectively (f_L and f_S for the average TGR were calculated as the average value between anaerobic and aerobic conditions, respectively); k_L and k_S are the rate constants for labile and stable DOM fractions, respectively, and they are calculated the same with f_L and f_S; and WRT_i is the corresponding hydrologic residence time at different elevations. Two assumptions have been made for this prediction model: (1) the submerging period equals the water residence time for each elevation and (2) submerged soil is the unique source for DOM to be biodegraded.

2.7. Statistics and QA/QC

All statistical analyses were performed using SPSS 23.0 software (IBM®, IL, USA). The Shapiro-Wilk method was used to test the normality of the data distribution. Both Spearman's r and Pearson's r were used in the correlation analysis; the former was used in the presence of non-normally distributed datasets (Shapiro-Wilk, $p < 0.05$), and the latter was used with normally distributed datasets (Shapiro-Wilk, $p > 0.05$). Automatic linear modelling was conducted to identify the important contributors from optical indices to DOM biodegradation (final to intial DOC in %). The forward stepwise method was used in variable picking. Variables entered into the model are probability-of-F-to-enter ≤ 0.05; variables removed from the model are probability-of-F-to-remove ≥ 0.10. Interactive effects of the DOM sources, degradation time and degradation conditions were compared by two-way ANOVA with Tukey's post-hoc tests. Significant differences among groups were tested by using both parametric (normally distributed) and non-parametric (not normally distributed) methods. Statistical significance (p) was determined at 0.05 and 0.01 (2-tailed). All results are reported as the mean ± standard deviation for three replicates. Noninoculated Milli-Q® water blanks for DOC analysis in the biodegradation experiment were subtracted by each treatment. Signals from Milli-Q® water blanks in spectra scans were subtracted automatically by Aqualog® EEM data processing software (*i.e.*, to remove the interferences of water Raman peaks). The detection limit for DOC is 0.5 mg L^{-1}. The relative standard deviations (RSD) in DOC measurement were all below 7%.

3. Results

3.1. DOM biodegradation

After incubation (28 days), the average DOC concentrations decreased from 16.2 ± 1.12 mg L^{-1} to 9.79 ± 0.78 mg L^{-1} under anaerobic conditions, and from 17.8 ± 0.98 mg L^{-1} to 7.90 ± 0.78 mg L^{-1} under aerobic conditions (Fig. 1a). Therefore, the total biodegraded DOM accounted for 39.5 ± 4% and 55.5 ± 6% in anaerobic and aerobic conditions, respectively (Fig. 1b). DOM from all sites (*i.e.*, FL, SB, TJ and KX) showed significantly higher degradation under aerobic than anaerobic conditions (Table S1, paired samples *t*-test, $p < 0.05$). However, the DOM degradability changed across sites. For example, DOM biodegradation at KX accounted for 33.5 ± 3% and 46.4 ± 2% DOM under anaerobic and aerobic conditions, respectively, and was, significantly lower than the other studied sites (Table S1, one-way ANOVA, $p < 0.05$). Two-way ANOVA showed that the incubation conditions (*i.e.*, anaerobic and aerobic) were more important than the DOM spatial distribution (*i.e.*, sampling sites) (Table S1, $p < 0.01$).

3.2. Kinetic model for DOM biodegradation

The kinetics of DOM biodegradation could be fit by a two-fraction first-order model (Table 1, adjusted $R^2 > 0.99$). Two fractions, including the labile DOM (low-molecular weight, usually it can decompose rapidly within weeks) and stable DOM (high-molecular weight, aromatic and humic-like), can be obtained from the fitting (Sondergaard and Middelboe, 1995; Kalbitz et al., 2003a). Under anaerobic conditions, the labile DOM fractions for different sites ranged from 14.1 ± 2 to 22.5 ± 3% (average 18.0 ± 14%) (Table 1). Under aerobic conditions, this amount increased from 33.8 ± 11 to 38.7 ± 3% (average 35.0 ± 2%) (Table 1). When comparing anaerobic and aerobic conditions, higher labile DOM fractions (paired samples t-test, $p < 0.01$) but lower k_1 values (not significant, $p = 0.14$) were found in aerobic conditions; on the contrary, higher stable DOM fractions (paired samples t-test, $p < 0.01$) but lower k_2 values (not significant, $p = 0.07$) were found in anaerobic conditions (Table 1).

3.3. Optical properties

Optical properties including the CDOM/DOC, SUVA$_{254}$, S$_{275-295}$ and S$_R$ were calculated by UV–vis absorption spectra (Fig. 2a–d). For the four studied sites, the average CDOM/DOC and SUVA$_{254}$ during all biodegradation kinetics were significantly higher in soil-extracted DOM incubated under aerobic conditions than in soil DOM incubated
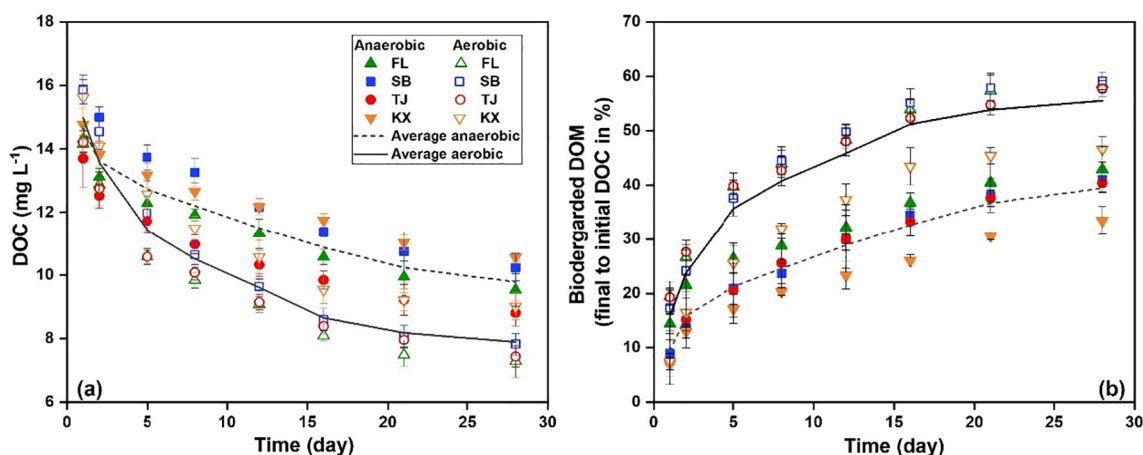

Fig. 1. Variations in the DOC concentrations (a) and biodegraded DOM with time (b). Error bars represent the standard deviation for three replicates.

Table 1
Parameters from the two-fraction first-order kinetic fitting of DOC degradation[*].

DOM sources	Incubation conditions	Biodegraded DOM (%)	Labile DOM fraction			Stable DOM fraction			R^2
			f_A (%)	k_1 (d^{-1})	Half-life (d)	f_B (%)	k_2 (d^{-1})	Half-life (d)	
FL	Anaerobic	$42.9 \pm 4\beta$	22.5 ± 3	0.98 ± 0.2	0.7	77.5 ± 3	0.011 ± 0.001	61.2	0.997
	Aerobic	$58.6 \pm 2\alpha$	37.1 ± 4	0.60 ± 0.1	1.2	62.9 ± 3	0.017 ± 0.002	41.3	0.995
SB	Anaerobic	$41.1 \pm 2\beta$	17.8 ± 2	0.60 ± 0.3	1.2	82.2 ± 2	0.013 ± 0.001	58.9	0.994
	Aerobic	$59.2 \pm 2\alpha$	38.7 ± 3	0.48 ± 0.2	1.1	61.3 ± 3	0.017 ± 0.004	44.7	0.994
TJ	Anaerobic	$40.4 \pm 1\beta$	18.5 ± 9	0.60 ± 0.2	1.2	81.5 ± 9	0.012 ± 0.005	53.7	0.995
	Aerobic	$57.8 \pm 1\alpha$	36.8 ± 4	0.64 ± 0.04	1.4	63.2 ± 4	0.016 ± 0.003	41.6	0.998
KX	Anaerobic	$33.5 \pm 3\beta$	14.1 ± 2	0.72 ± 0.1	1.0	85.9 ± 2	0.009 ± 0.002	72.7	0.997
	Aerobic	$46.6 \pm 2\alpha$	33.8 ± 11	0.29 ± 0.1	2.4	66.2 ± 11	0.009 ± 0.007	74.1	0.994
Average anaerobic		$39.5 \pm 4\beta$	18.0 ± 1	0.68 ± 0.1	1.0	82.0 ± 1	0.012 ± 0.001	57.8	0.995
Average aerobic		$55.5 \pm 6\alpha$	35.0 ± 2	0.50 ± 0.1	1.4	65.0 ± 2	0.015 ± 0.002	46.2	0.994

[*] Mean $\pm$ SD ($n = 3$). Biodegraded DOM was expressed as final to initial DOC in %; f_A and f_B are the fractions of labile DOM and stable DOM; k_1 and k_2 are the degradation rate constants for labile and stable DOM fractions, respectively. Different Greek letters in the biodegraded DOM column indicate that the difference between anaerobic and aerobic conditions is significant (t-test, $p < 0.05$).

under anaerobic conditions ($p < 0.05$, Fig. 2a and b). Moreover, we observed the same trend when considering all of the sites together. No significant difference in $S_{275-295}$ (Fig. 2c) and S_R (Fig. 2d) between the two incubation conditions was found (with only one exception of S_R in the KX treatment). The ranges of $S_{275-295}$ in DOM biodegradation are relatively narrow, and most $S_{275-295}$ values range between 0.015 and 0.020 (nm^{-1}). The kinetic variations of CDOM/DOC, SUVA$_{254}$, $S_{275-295}$ and S_R are shown in Fig. S2.

Four fluorescence compounds were identified from the fluorescence spectra as one humic-like compound (peak A), one fulvic-like

compound (peak C) and two protein-like compounds (peak B and peak T). During the kinetic experiment, the average intensities of peak A and peak C in aerobic treatments were all higher than those in anaerobic treatments ($p < 0.05$, Fig. 2e and f). High variations were found for the intensities of protein-like peaks (peak B and peak T) due to the larger ranges in box plots (Fig. 2g and h). A significantly higher intensity of peak B was only found in aerobic treatment of the TJ site ($p < 0.05$). Despite the visual difference of peak B and T intensities between aerobic and anaerobic conditions at the four sites (FL, SB, KX and TJ), the statistical test indicated that these differences were not significant. However,
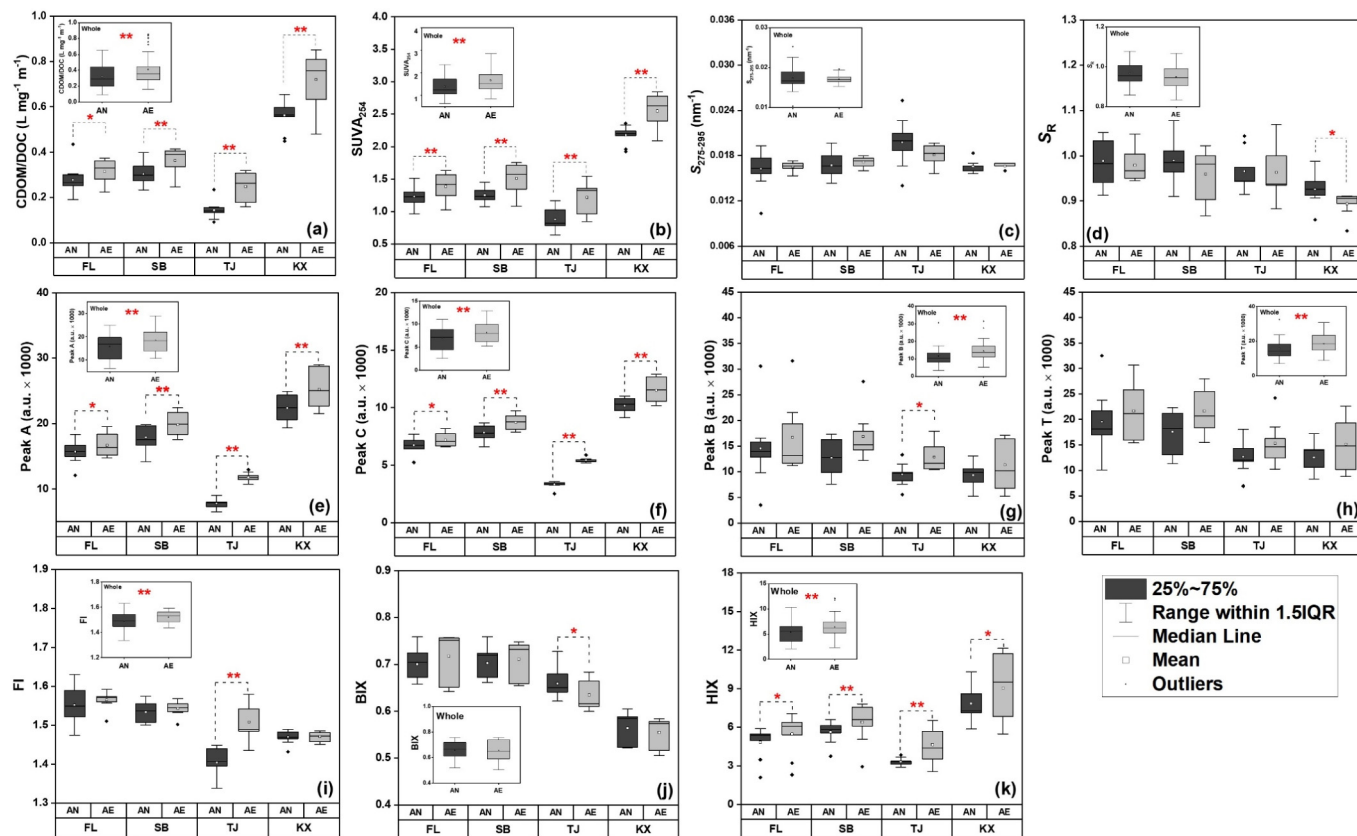

Fig. 2. Optical properties of DOM in biodegradation. (a) CDOM/DOC; (b) SUVA$_{254}$; (c) $S_{275-295}$; (d) S_R; (e) Peak A for humic-like compound; (f) Peak C for fulvic-like compound; (g) Peak B and (h) Peak T for protein-like compounds; (i) FI; (j) BIX and (k) HIX. Data for each box in the main plot included all the data points in biodegradation kinetics ($n = 9$, from day 0 to day 28). The subgraphs in each plot are the combined datasets from the four sites and referred to as the whole TGR condition ($n = 32$). FL, SB, TJ and KX are the four sampling sites; AN and AE indicate anaerobic and aerobic conditions, respectively. "*" or "**" indicates that the difference between aerobic and anaerobic conditions is significant at $p < 0.05$ or $p < 0.01$ through the paired samples t-test. IQR indicates the interquartile range.

when taking all the sites together, the peak B and peak T intensities were significantly higher under aerobic conditions than under anaerobic conditions ($p < 0.01$, Fig. 2g and h). On day 28, a significant difference in the peak B intensity was found at the TJ site ($p < 0.05$), whereas for the peak T intensity, significant differences were found at the FL, SB and KX sites ($p < 0.05$). Fluorescence indices including FI, BIX and HIX were calculated. In general, FI was higher in aerobic treatments than in anaerobic treatments; however, a significant difference was only found in TJ soil-extracted DOM ($p < 0.01$, Fig. 2i). Higher BIX values were found in the anaerobic treatments of site TJ than in the aerobic treatments ($p < 0.05$, Fig. 2j). HIX values were also higher in aerobic treatments than in anaerobic treatments ($p < 0.05$, Fig. 2k). Variations in the fluorescence peak intensities (*i.e.*, peak A, C, B, and T) and fluorescence indices (*i.e.*, FI, BIX, and HIX) can be found in Figs. S3 and S4, respectively.

3.4. Correlations between biodegraded DOM and the optical properties

Correlations between the biodegraded DOM (final to initial DOC in %) and the optical properties were carried out in both anaerobic and aerobic condition treatments during biodegradation (*i.e.*, data points from the kinetics experiment, $n = 27$). From the UV–vis absorption properties, $SUVA_{254}$ and CDOM/DOC were found to be positively correlated with biodegraded DOM in all treatments and the average TGR region (represented by four sites averaged data) (Table 2, $p < 0.05$). Moreover, the correlation coefficients of $SUVA_{254}$ and CDOM/DOC were higher in aerobic treatments than in anaerobic treatments (with the exceptions of $SUVA_{254}$ for KX and the average TGR). The amount of CDOM (reflected by a_{355}) showed a negative correlation with the biodegraded DOM in aerobic treatments (Table 2, $p < 0.05$), but no significant correlations were found in any of the anaerobic treatments (Table 2). The intensities of peak A and C are negatively correlated with the biodegraded DOM (Table 2, $p < 0.05$), but BIX and HIX are positively correlated with the biodegraded DOM under both anaerobic and aerobic conditions with only one exception (KX DOM under anaerobic conditions) (Table 2, $p < 0.05$).

3.5. DOM biodegradation potential in the WLFZ of the TGR region

Prediction lines were plotted for anaerobic, aerobic and the average of anaerobic and aerobic conditions (Fig. 3a). Under anaerobic conditions, the DOM released from submerged soils could be biodegraded by 66.5%, 78.5% and 81.0% at 170 m, 160 m and 150 m elevations,

respectively. These values will increase to 76.5%, 85.4% and 87.2% under aerobic conditions for the same elevations, respectively. It is recognized that the average between anaerobic and aerobic conditions (*i.e.*, the average TGR in Fig. 3a) is closer to the real WLFZ in the TGR region. This is because the real redox conditions in the WLFZ elevations fluctuate greatly, and the biodegradation of soil-released DOM could either proceed under aerobic or anaerobic conditions during flooding. On average, 71.2%, 81.7%, and 84.0% of DOM leached from submerged soil could be biodegraded at 170 m, 160 m and 150 m elevations of the WLFZ, respectively (Fig. 3a).

4. Discussion

4.1. DOM biodegradation in general

Biodegradation is one of the key pathways of DOM depletion in natural environments (Marschner and Kalbitz, 2003; Cory and Kling, 2018). Microorganism-mediated DOM losses and transformation have significant influences on the environmental behaviours of DOM and carbon cycling (Berggren et al., 2010). Regarding the length of kinetic degradation experiments, short-term compared to long-term (*e.g.*, year) studies are more important because the rates of microbial response to DOM degradation are typically rapid (*e.g.*, minutes to days) (Cory and Kling, 2018). In this short-term study, the biodegraded DOM was, on average, $47.5 \pm 10\%$ ($n = 24$) independent of the treatments. This value is similar to the DOM biodegradation from other hydrology influencing regions, such as the Yongjiang River and Fluvià River (Table S2), but higher than the DOM extracted from soils with similar climates (Liu et al., 2019a) or soils from agricultural fields (Kalbitz et al., 2003a). This highlighted the importance of hydrology alternation-induced wetland systems in soil organic carbon turnover. Moreover, the relative abundance of polymethylene chain compounds identified by pyrolysis-gas chromatography–mass spectrometry (Py-GC-MS) in a previous study (Jiang et al., 2017) correlated negatively with the biodegraded DOM ($r = -0.96$, $p < 0.05$ for anaerobic treatments; $r = -0.97$, $p < 0.05$ for aerobic treatments, Fig. S5a). This suggests that these compounds, which account for $12.6 \pm 2.5\%$ of DOM in the TGR region (Jiang et al., 2017) and are derived from aliphatic biopolymers such as cutin and suberin originating from vascular plants or algaenan in algae (Kaal et al., 2015), were resistant to biological degradation under either aerobic or anaerobic conditions.

In this study, the DOM fraction resistant to biological degradation (*i.e.*, refractory) had longer half-life values (41.3–74.1 d) and proportions

Table 2
Correlation coefficients between biodegraded DOM and the optical properties.

	FL[a]		SB[a]		TJ[a]		KX[a]		Average TGR[b]		Responses[c]
	Anaerobic	Aerobic	Anaerobic	Aerobic	Anaerobic	Aerobic	Anaerobic	Aerobic	Anaerobic	Aerobic	
$SUVA_{254}$	0.91	0.93	0.81	0.92	0.77	0.91	0.92	0.91	0.99	0.98	Significant
a_{355}	/	−0.81	/	−0.89	−0.61	−0.94	/	−0.94	/	−0.99	Significant
CDOM/DOC	0.81	0.88	0.73	0.82	0.60	0.86	0.67	0.86	0.88	0.97	Significant
$S_{275-295}$	−0.64	/	−0.48	/	−0.39	/	/	/	/	/	Non-significant
S_R	0.49	/	/	−0.69	/	/	/	/	/	/	Non-significant
Peak A	−0.75	−0.87	−0.81	−0.94	−0.86	−0.95	/	−0.95	−0.93	−0.98	Significant
Peak C	−0.80	−0.90	−0.89	−0.92	−0.86	−0.95	−0.44	−0.95	−0.93	−0.97	Significant
Peak B	−0.61	/	−0.56	/	−0.56	−0.79	/	−0.79	−0.80	−0.72	Non-significant
Peak T	−0.55	−0.54	/	−0.43	/	−0.55	/	−0.55	/	/	Non-significant
r(A/C)	−0.48	−0.61	−0.40	−0.80	−0.76	−0.81	/	−0.81	/	−0.98	Significant
r(T/C)	−0.47	/	/	/	/	/	/	/	/	/	Non-significant
FI	−0.63	/	/	/	/	0.61	/	0.61	/	0.75	Non-significant
BIX	0.81	0.79	0.80	0.80	0.82	0.87	0.68	0.87	0.97	0.99	Significant
HIX	0.55	0.79	0.69	0.91	0.74	0.89	/	0.89	0.90	0.99	Significant

Spearman's r was used in the correlation analysis. All of the numbers in the form indicate significant correlations ($p < 0.05$); "/" indicates that the correlation is not significant.

[a] FL, SB, TJ and KX indicate the DOM extracted from different soils. $n = 27$.

[b] Average TGR indicates correlations by using the averaged data from 4 sites. $n = 9$.

[c] Significant (or non-significant) indicates that the correlations are independent (or dependent) of the spatial distribution in the TGR region (*i.e.*, different sites).
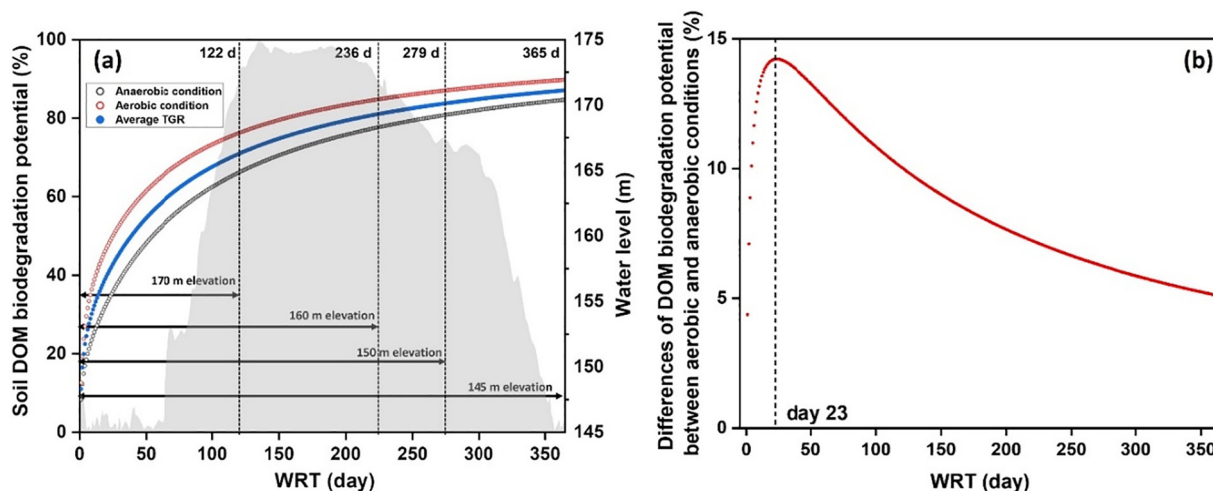
Fig. 3. Soil DOM biodegradation potential at different elevations (a) and differences in the DOM biodegradation potential between aerobic and anaerobic conditions (b, aerobic condition minus anaerobic condition). The black dashed lines in the (a) plot indicate the different WRTs for each elevation (*i.e.*, 170, 160, 150 and 145 m); the black dashed line in the (b) plot indicates the maximum value at day 23. The WRT for each elevation is from the average water level recorded before the TGR dam from 2013 to 2016, http://www.cjh.com.cn (≤ 145 m elevation, $WRT_{145} = 365$ d; 150 m elevation, $WRT_{150} = 279$ d; 160 m elevation, $WRT_{160} = 236$ d; 170 m elevation, $WRT_{170} = 122$ d). The shadow area indicates the water level changes from June 1st, 2015 to May 31st, 2016.

(from 61.3–85.9%) than the labile fraction (Table 1). This is because the origins of soil-extracted DOM at the WLFZ were mainly composed of terrigenous DOM, including the local soil organic matter pool and agricultural activity inputs (*e.g.*, organic fertilization and plant-derived organic matter). Contributions from water-borne DOM sedimentation during the flooding period (*e.g.*, microbial-derived organic matter) only account for a small proportion of the bulk soil-extracted DOM. This is consistent with our previous study that soil DOM in the TGR area showed both autochthonous and the allochthonous characteristics, and allochthonous character is dominant for most sites (Jiang et al., 2017, 2019).

4.2. Anaerobic versus aerobic biodegradation: labile and stable fractions

Similar to other regions with fluctuating hydrology, oscillations in the redox conditions occur frequently in the WLFZ of the TGR region due to the nonseasonal water level changes caused by artificial hydrological adjustment (Bao et al., 2015). As a result, soil DOM might be biodegraded under both aerobic and anaerobic conditions. In this study, more DOM could be aerobically biodegraded (Fig. 1, Table S1), which is consistent with studies from others (Bastviken et al., 2004; Reimers et al., 2013; Fasching et al., 2014; Seidel et al., 2014; Liu et al., 2019a). In the water column or sediment, labile DOM in both anaerobic and aerobic conditions is equally accessible to enzymes and could be depleted first. However, some recalcitrant DOM can only be available to oxygenases or reactive oxygen species (Bastviken et al., 2004). Therefore, the degradation of the stable DOM fraction may be limited to anaerobic environments (Middelburg, 1989; Koehler et al., 2012).

Theoretically, for a given microbial community, labile (f_A) and recalcitrant (f_B) DOM fractions from a given site should be constant. In this study, for the same microbial inoculum and same soil extracted DOM we obtained different f values under aerobic and anaerobic conditions (Table 1) (t-test, $p < 0.05$). This suggests that O_2 controlled the accessibility of the microbial community to different DOM fractions. The dominant species of heterotrophic microorganisms, which mediate the majority of DOM biodegradation, may be different under aerobic and anaerobic conditions (Berggren et al., 2010; Kamjunke et al., 2016). Moreover, O_2 is likely preferentially used as a terminal electron acceptor (TEA) for DOM degradation under aerobic conditions (LaRowe and Van Cappellen, 2011; Chen and Hur, 2015), resulting in CO_2 formation (Gao et al., 2019). In anaerobic environments, however, the TEA will shift from O_2 to other compounds (*e.g.*, NO_3^-, SO_4^{2-} and Fe^{3+}) and result in

different DOM degradation rates according to the different metabolic potentials (Chen and Hur, 2015; Derrien et al., 2019).

However, in our study, higher k_1 values were found under anaerobic conditions compared to aerobic conditions ($p < 0.05$, with the exception of the TJ), whereas higher k_2 values were found in aerobic conditions (only FL, $p < 0.05$) (Table 1). Although the differences in the average k_1 between the two conditions (average for the four sites) are not significant, it still suggests that the biodegradation rate of labile DOM may be faster (or at least as fast) under anaerobic conditions as under aerobic conditions. Through an anoxic and oxic rotated incubation, Bastviken et al. (2004) identified that 16–18% degradable DOM could be degraded more rapidly under anoxic conditions than under oxic conditions. This highlights the role of anaerobic DOM degradation in the carbon cycle. In contrast, the biodegradation rate of stable DOM seems to be faster in aerobic conditions than anaerobic conditions (Table 1). Nevertheless, the negative correlation between lignin products identified previously (Jiang et al., 2017) and k_1 in aerobic treatments ($r = -0.99$, $p < 0.01$, Fig. S5b) suggests that lignin decomposition may be a rate-limiting step in aerobic conditions. Indeed, several studies have shown that lignin could only be depolymerized by extracellular enzymes from a few microorganisms (Austin and Ballaré, 2010).

4.3. Anaerobic versus aerobic biodegradation: optical properties

A simple correlation between the DOM biodegradation (in %) and the original optical properties of soil DOM from four sites was conducted. Only a few original optical indices or peaks were significantly correlated with the biodegraded DOM (Table S3). This implies that the differences in the properties of original DOM may not be used to predict to what extent DOM might be biodegraded (similar to our two-way ANOVA test result in Table S1). Unlike Fellman et al. (2009), who used protein-like fluorescence compounds and $SUVA_{254}$ to predict the soil DOM biodegradation potential, this work implies that the optical properties of DOM will change dynamically during either anaerobic or aerobic biodegradation. Thus, the changes in the optical properties of DOM during the kinetic experiment (instead of the original optical properties) were used to reflect the compositional changes of SOM in biodegradation.

Overall, in terms of the average rate of change during the entire kinetic period, higher values of normalized CDOM (*i.e.*, CDOM/DOC), $SUVA_{254}$, intensities of peak A and peak C, and HIX were found in all

aerobic treatments compared to the other parameters (Fig. 2a, b, e, f and k), suggesting a higher processing of the labile DOM and further concentration of the recalcitrant DOM fraction. This enhancement of condensed aromatic structures of DOM has also been named "microbial humification" (Lee et al., 2018). The labile fraction of DOM (*i.e.*, low-molecule weight, aliphatic) is first consumed by microorganisms in either aerobic or anaerobic conditions (Pellerin et al., 2010; Hansen et al., 2016). Then, the utilization of some less recalcitrant DOM by heterotrophic bacteria could be promoted by oxygen attack (Marschner and Kalbitz, 2003; Bastviken et al., 2004; Reimers et al., 2013). The remaining DOM, which cannot be degraded further by microorganisms in aerobic conditions, is usually considered highly recalcitrant and could be coagulated by self-assembly (Xu and Guo, 2018). Irrespective of the sampling sites, positive correlations of SUVA$_{254}$ *versus* CDOM based on the overall dataset were found in both anaerobic ($r = 0.93$, $p < 0.001$, Fig. 4a) and aerobic ($r = 0.79$, $p < 0.001$, Fig. 4b) conditions, suggesting that chromophores are associated with aromaticity in WLFZ soil DOM biodegradation. This is in line with our previous monitoring of the aquatic DOM in the TGR during both the dry and wet seasons, in which the changes in chromophoric components are related to changes in aromaticity (Jiang et al., 2018b). However, the significant correlations between SUVA$_{254}$ and CDOM were site-dependent under aerobic conditions. Negative correlations in sites FL, SB, and KX (Fig. 4b) along the kinetic experiments (*i.e.*, time-series data for these sites) suggest that some chromophores were also depleted in aerobic biodegradation although the bulk aromaticity increased. This means that the CDOM was also concentrated during aerobic biodegradation. Exponential coupling of DOC and CDOM was found in aerobic conditions (CDOM in FL, SB and KX explained 87%, 86% and 89% of DOC variations) but absent in anaerobic conditions (Fig. S6), which suggests that the depletion of DOC was faster than the degradation of CDOM at the earlier stages of aerobic biodegradation. This coupling further explains why CDOM in aerobic biodegradation could either be concentrated (*i.e.*, positive correlation between biodegraded DOM and CDOM/DOC, Table 2) or depleted (*i.e.*, negative correlation between biodegraded DOM and *a*(355), Table 2; negative correlations between *a*(355) and SUVA$_{254}$, Fig. 4b). Moreover, the coupling between DOC and CDOM in aerobic biodegradation could provide a simple test to rapidly estimate DOC concentrations in the flooding water of the TGR though only measuring the filtered water color.
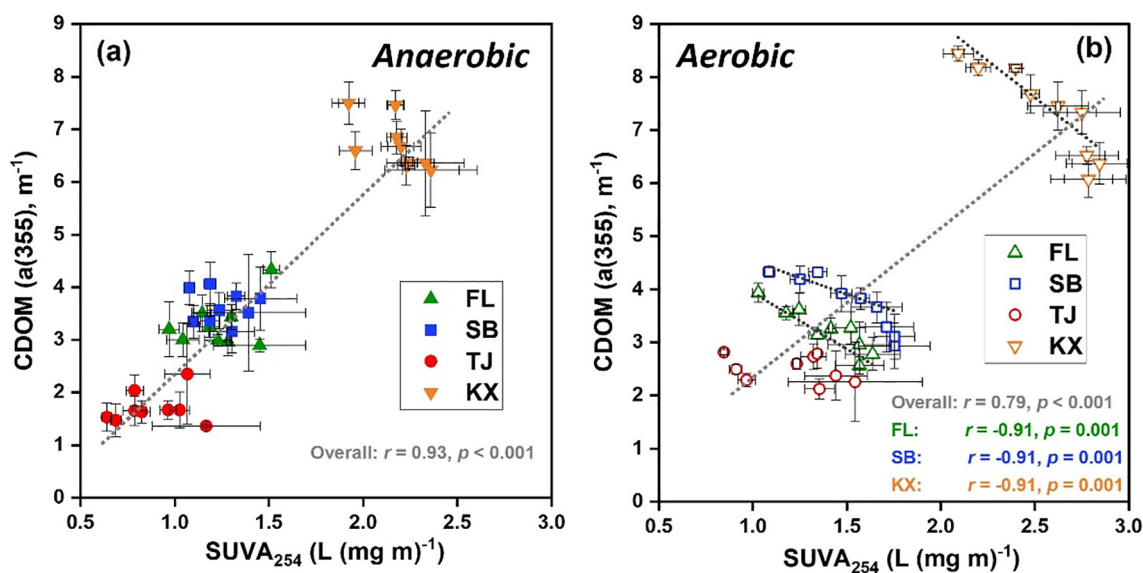
Differences in other optical properties, such as $S_{275-295}$, S_R, intensities of peak B and peak T, FI and BIX, in anaerobic and aerobic conditions were not statistically significant (Fig. 2c, d, g, h, i and j). This indicates that the responses of molecular weight (reflected by $S_{275-295}$ and S_R, Helms et al., 2008; Hur et al., 2009) and autochthonous signals of DOM in degradation in different oxygen regimes are less sensitive than the aromaticity and allochthonous signals of DOM. In contrast to the continuous decrease reported by Hansen et al. (2016), in this study, the dynamics of $S_{275-295}$ (Fig. S2c) and S_R (Fig. S2d) varied. Some increases in $S_{275-295}$ and S_R, especially under aerobic conditions, indicate the following: (1) losses of higher molecular weight DOM due to disaggregation or bond cleavage and (2) increases in low-molecular weight DOM production through metabolism (Stepanauskas et al., 2005). The dynamics of two autochthonous protein-like compounds (peak B for tyrosine-like compounds and peak T for tyrptophane-like compounds) also support that more signals from microbially-derived DOM are involved in biodegradation (Fig. S3c and S3d) (Coble, 1996; Coble, 2007). Some extracellular enzymes and metabolic products (*i.e.*, low-molecular weight DOM) may be released simultaneously (Seidel et al., 2014; Autio et al., 2016).

It should be noted that the above analysis of this study is based on a limited number of samples collected from TGR areas, and thus, we hesitate to extend too much for discussing the change trend of DOM properties in a specific (*i.e.*, individual) site. However, it is useful to have a preliminary impression as a whole for extrapolating the DOM degradation in TGR areas.

4.4. Contribution of optical properties to DOM under aerobic and anaerobic incubation conditions

To track the contributions of DOM optical properties to its biodegradation capacities under aerobic *versus* anaerobic incubation conditions, automatic linear modelling with the forward stepwise method was conducted on four sites (combined data, Fig. 5). Only significant properties (*i.e.*, correlations with biodegraded DOM are independent of sites under either anaerobic or aerobic conditions, Table 2) were input as variables for the regression. In anaerobic conditions, SUVA$_{254}$ and BIX are the dominant predictors (importance larger than 0.3), whereas the importance values of other properties are smaller than 0.1 (Fig. 5a). Under aerobic conditions, SUVA$_{254}$ is the absolute predominant factor
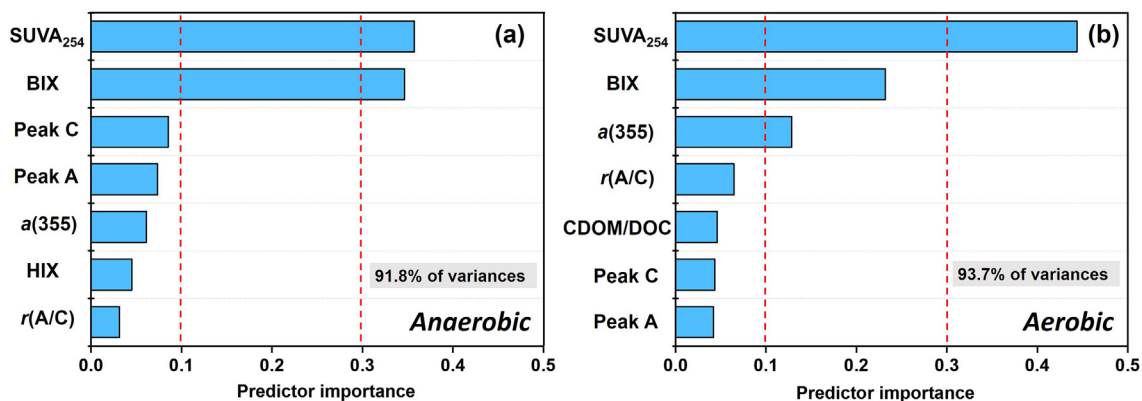

Fig. 4. SUVA$_{254}$ *versus* CDOM in anaerobic (a) and aerobic (b) conditions. Kinetic data for each site were used ($n = 9$ for each site). Spearman's r was used for correlations, and the significance level was $p < 0.05$. Short dotted lines indicate a significant correlation. Error bars in the vertical and horizontal directions are the standard deviation (SD) from three replicates of CDOM and SUVA$_{254}$, respectively.

Fig. 5. Predictor importance from linear forward stepwise modelling in anaerobic (a) and aerobic (b) conditions by using the combined data of four sites. Accuracy indicates the degree of explanation obtained from modelling. The red dashed lines are the cutoffs for highly important predictors (> 0.3), important predictors (0.1–0.3) and less important predictors (< 0.1).

(importance of 0.44), followed by BIX and a(355) (Fig. 5b). According to the linear modelling, SUVA$_{254}$ and BIX show high contributions to DOM biodegradation under either anaerobic or aerobic conditions, which agrees with Lee et al. (2018). The close association between SUVA$_{254}$ and DOM biodegradation (Fig. S7) further supports the preferential microbial removal of labile DOM (Hur et al., 2011; Hansen et al., 2016). The contribution from BIX suggests that the biodegradation of soil DOM is a partial degradation (Berggren et al., 2010; Zheng et al., 2014; Cory and Kling, 2018), and some stable DOM was biodegraded into lower molecular or aliphatic compounds, instead of CO_2. However, in some anoxic conditions such as the flooding period in the WLFZ of the TGR, the contribution to DOM biodegradation from CDOM will increase. Thus, water colour changes may be used as an indicator to track the oxygen regimes of submerged soil in the WLFZ of the TGR region. In addition, the changes in two parameters, HIX in the anaerobic treatment and CDOM/DOC in the aerobic treatment (Fig. 5), are specific to the response to the two different degradation conditions. Thus, they might be used to distinguish the two distinct degradation conditions.

On the other hand, we should note the limits of optical analysis used in this study, which reflects only a small portion of the bulk DOM (optically active components). However, previous studies illustrated that the optical indices showed good correlation with molecular formula interpretations derived from ultra high resolution mass spectrometry (FTICR-MS) (Wagner et al., 2015; Kellerman et al., 2018). Sleighter et al. (2014) also found consistency between optical and FTICR-MS data and importantly, two categories of methods showed that the corroboration between optical and FTICR-MS data of labile and semi-labile DOM, which is consistent with the component of DOM susceptible to microbial degradation (Kim et al., 2006; Ward et al., 2013; Sleighter et al., 2014). Additionally, considering the studies on DOM biodegradation using mass techniques, the observation of DOM bioreactivities aligned with formula identifiers were not consistent (Sleighter et al., 2014). This discrepancy indicates the limits of FTICR-MS, which can provide compositional information on the DOM but not about structures which are also key players that attribute to the bioreactivity (Sleighter et al., 2014). Thus, this study highlights the utility of simple and inexpensive measurements (*i.e.*, absorbance and fluorescence measurements) for assessing the DOM cycle, especially bioreactivity, in aquatic environments.

4.5. DOM biodegradation potential in the WLFZ of the TGR region

In this study, the results of biodegraded DOM (%) among the four sampling sites were found within a relatively small range (33.5–42.9% for anaerobic conditions and 46.6–59.2% for aerobic conditions, Table 1). This suggests that the bioreactivities of soil DOM at these

sites (*i.e.*, FL, SB, TJ, and KX) of the TGR region might be constrained to a relatively narrow ranges. Therefore, a regional prediction of soil DOM biodegradation potential was simply conducted based on the four sites (Fig. 3). The largest difference in the DOM biodegradation potential between aerobic and anaerobic conditions was found in the WRT at 23 days (the difference is 14.2%), and this value decreased with increasing WRT (Fig. 3b). This indicates that hydrologic conditions regulate soil DOM biodegradation and that anaerobic biodegradation cannot be overlooked. It should be emphasized that the real water residence time at each elevation is usually shorter than the flooding time (especially in the mainstream of the Yangtze River, sites FL and KX in this study). The prediction results in this model may overestimate the biodegradability of DOM in the TGR region to a certain degree. However, it provides a preliminary quantitative understanding of the microbe-mediated DOM loss from submerged soils in the WLFZ of the TGR annually. Other geochemical factors, instead of oxygen regimes and hydrologic conditions, could also influence the DOM biodegradation potential. Temperature is thought to be one of the most important factors influencing soil DOM biodegradation (Marschner and Kalbitz, 2003; Evans et al., 2017). Importantly, refractory organic matter could be decomposed more rapidly by labile organic carbon addition under oxic conditions (Guenet et al., 2010, 2014). Thus, the alternation of wet-dry conditions in TGR areas might enhance DOM biodegradation when the water level decreases. Furthermore, DOM bioavailability can influence the environmental fate of contaminants, such as Hg. Although the higher degradation potential of DOM in aerobic conditions (*e.g.*, shallow waters) observed in this study may enhance microbial growth, the Hg methylation could be offset by the inhibition of aerobic conditions on anaerobic bacteria (*e.g.*, iron- or sulfur-reducing bacteria). Thus, the results found in this study will be used as a basis for further investigations on the influences of DOM degradation under anaerobic and aerobic conditions on Hg methylation by bacteria.

5. Conclusions

This study examined the anaerobic and aerobic biodegradation of water-extracted soil DOM from the WLFZ of the TGR region. While DOM biodegradation was higher under aerobic conditions than under anaerobic conditions, anaerobic DOM processing contributed up to 40% of the total DOM degradation. Our results show that while labile DOM was biologically degraded under both aerobic and anaerobic conditions, recalcitrant DOM was degraded mainly under aerobic conditions. Consequently, the DOM optical properties indicated that soil-extracted DOM incubated under aerobic conditions was enriched in recalcitrant DOM and depleted in labile DOM. Our results demonstrate that anaerobic DOM processing might be a highly relevant DOM

degradation process, especially in the water level fluctuation areas of large reservoirs such as the TGR. Lastly, this study notes that the management of reservoir water flow and the subsequent changes in the hydrologic conditions of reservoirs regulate soil DOM biodegradation and might thus have an important impact on the global carbon cycle.

CRediT authorship contribution statement

Jiang Liu: Methodology, Software, Investigation, Data curation, Formal analysis, Writing - original draft. **Jian Liang:** Investigation, Data curation, Formal analysis, Writing - original draft. **Andrea G. Bravo:** Methodology, Formal analysis, Writing - review & editing. **Shiqiang Wei:** Writing - review & editing, Investigation. **Caiyun Yang:** Methodology, Formal analysis, Writing - review & editing. **Dingyong Wang:** Conceptualization, Methodology, Formal analysis, Writing - review & editing. **Tao Jiang:** Supervision, Conceptualization, Methodology, Investigation, Formal analysis, Writing - review & editing.

Declaration of competing interest

The authors declare that they have no known competing financial interests or personal relationships that could have appeared to influence the work reported in this paper.

Acknowledgement

Appendix A. Supplementary data

Supplementary data to this article can be found online at https://doi.org/10.1016/j.scitotenv.2020.142857.

References

Aiken, G.R., Gilmour, C.C., Krabbenhoft, D.P., Orem, W., 2011. Dissolved organic matter in the Florida Everglades: implications for ecosystem restoration. Crit. Rev. Environ. Sci. Technol. 41, 217–248.

Austin, A.T., Ballaré, C.L., 2010. Dual role of lignin in plant litter decomposition in terrestrial ecosystems. Proc. Natl. Acad. Sci. U. S. A. 107 (10), 4618–4622.

Autio, I., Soinne, H., Helin, J., Asmala, E., Hoikkala, L., 2016. Effect of catchment land use and soil type on the concentration, quality, and bacterial degradation of riverine dissolved organic matter. Ambio 45 (3), 331–349.

Bao, Y.H., Gao, P., He, X.B., 2015. The water-level fluctuation zone of three gorges reservoir - a unique geomorphological unit. Earth Sci. Rev. 150, 14–24.

Bastviken, D., Persson, L., Odham, G., Tranvik, L., 2004. Degradation of dissolved organic matter in oxic and anoxic lake water. Limnol. Oceanogr. 49 (1), 109–116.

Berggren, M., Laudon, H., Haei, M., Stro, L., 2010. Efficient aquatic bacterial metabolism of dissolved low-molecular-weight compounds from terrestrial sources. ISME J. 4, 408–416.

Bravo, A.G., Bouchet, S., Tolu, J., Björn, E., Mateos-Rivera, A., Bertilsson, S., 2017. Molecular composition of organic matter controls methylmercury formation in boreal lakes. Nat. Commun. 8, 14255.

Burdige, D.J., 2007. Preservation of organic matter in marine sediments: controls, mechanisms, and an imbalance in sediment organic carbon budgets? Chem. Rev. 107, 467–485.

Chen, M., Hur, J., 2015. Pre-treatments, characteristics, and biogeochemical dynamics of dissolved organic matter in sediments: a review. Water Res. 79, 10–25.

Coble, P.G., 1996. Characterization of marine and terrestrial DOM in seawater using excitation emission matrix spectroscopy. Mar. Chem. 51, 325–346.

Coble, P.G., 2007. Marine optical biogeochemistry: the chemistry of ocean color. Chem. Rev. 107, 402–418.

Coble, P.G., Spencer, R.G.M., Baker, A., Reynolds, D.M., 2014. Aquatic organic matter fluorescence. In: Coble, P.G., Lead, J., Baker, A., Reynolds, D.M., Spencer, R.G.M. (Eds.), Aquatic Organic Matter Fluorescence. Cambridge University Press, US, pp. 75–122.

Cory, R.M., Kaplan, L.A., 2012. Biological lability of streamwaer fluorescent dissolved organic matter. Limnol. Oceanogr. 57, 1347–1360.

Cory, R.M., Kling, G.W., 2018. Interactions between sunlight and microorganisms influence dissolved organic matter degradation along the aquatic continuum. Limnol. Oceanogr. Lett. 3, 102–116.

Derrien, M., Shin, K., Hur, J., 2019. Biodegradation-induced signatures in sediment pore water dissolved organic matter: implications from artificial sediments composed of two contrasting sources. Sci. Total Environ. 694, 133714.

Evans, C.D., Futter, M.N., Moldan, F., Valinia, S., Frogbrook, Z., Kothawala, D.N., 2017. Variability in organic carbon reactivity across lake residence time and trophic gradients. Nat. Geosci. 10, 832–835.

Fasching, C., Behounek, B., Singer, G.A., Battin, T.J., 2014. Microbial degradation of terrigenous dissolved organic matter and potential consequences for carbon cycling in brown-water streams. Sci. Rep. 4, 4981.

Fasching, C., Akotoye, C., Bi, M., Fonvielle, J., Ionescu, D., Mathavarajah, S., Zoccarato, L., Walsh, D.A., Grossart, H., Xenopoulos, M.A., 2020. Linking stream microbial community functional genes to dissolved organic matter and inorganic nutrients. Limnol. Oceanogr. 65, S71–S87.

Fellman, J.B., Hood, E., D'Amore, D.V., Edwards, R.T., White, D., 2009. Seasonal changes in the chemical quality and biodegradability of dissolved organic matter exported from soils to streams in coastal temperate rainforest watershed. Biogeochemistry 95, 277–293.

Gao, C., Sander, M., Agethen, S., Knorr, K.H., 2019. Electron accepting capacity of dissolved and particulate organic matter control CO_2 and CH_4 formation in peat soils. Geochem. Cosmochim. Acta 245, 266–277.

Grasset, C., Mendonc, R., Saucedo, G.V., Bastviken, D., Roland, F., Sobek, S., 2018. Large but variable methane production in anoxic freshwater sediment upon addition of allochthonous and autochthonous organic matter. Limnol. Oceanogr. 63 (4), 1488–1501.

Guenet, B., Danger, M., Abbadie, L., Lacroix, G., 2010. Priming effect: bridging the gap between terrestrial and aquatic ecology. Ecology 91, 2850–2861.

Guenet, B., Danger, M., Harrault, L., Allard, B., Jauset-Alcala, M., Bardoux, G., Benest, D., Abbadie, L., Lacroix, G., 2014. Fast mineralization of land-born C in inland waters: first experimental evidences of aquatic priming effect. Hydrobiologia 721, 35–44.

Hansen, A.M., Kraus, T.E.C., Pellerin, B.A., Fleck, J.A., Downing, B.D., Bergamaschi, B.A., 2016. Optical properties of dissolved organic matter (DOM): effects of biological and photolytic degradation. Limnol. Oceanogr. 61, 1015–1032.

Helms, J.R., Stubbins, A., Ritchie, J.D., Minor, E.C., Kieber, D.J., Mopper, K., 2008. Absorption spectral slopes and slope ratios as indicators of molecular weight, source, and photobleaching of chromophoric dissolved organic matter. Limnol. Oceanogr. 53 (3), 955–969.

Herrero Ortega, S., Catalán, N., Björn, E., Gröntoft, H., Hilmarsson, T.G., Bertilsson, S., Wu, P., Bishop, K., Levanoni, O., Bravo, A.G., 2017. High methylmercury formation in ponds fueled by fresh humic and algal derived organic matter. Limnol. Oceanogr. 63, S44–S53.

Hongve, D., van Hees, P.A.W., Lundstrom, U.S., 2000. Dissolved components in precipitation water percolated through forest litter. Eur. J. Soil Sci. 51, 667–677.

Hur, J., Park, M.H., Schlautman, M.A., 2009. Microbial transformation of dissolved leaf litter organic matter and its effects on selected organic matter operational descriptors. Environ. Sci. Technol. 43, 2315–2321.

Hur, J., Lee, B.M., Shin, H.S., 2011. Microbial degradation of dissolved organic matter (DOM) and its influence on phenanthrene-DOM interactions. Chemosphere 85, 1360–1367.

Jansen, B., Kalbitz, K., McDowell, W.H., 2014. Dissolved organic matter: linking soils and aquatic systems. Vadose Zone J. 13 (7).

Jiang, T., Kaal, J., Liu, J., Liang, J., Zhang, Y., Wang, D., 2020a. Linking the electron donation capacity to the molecular composition of soil dissolved organic matter from the Three Gorges Reservoir areas, China. J. Environ. Sci. 90, 146–156.

Jiang, T., Skyllberg, U., Wei, S., Wang, D., Lu, S., Jiang, Z.M., Flanagan, D.C., 2015. Modeling of the structure-specific kinetics of abiotic, dark reduction of hg(II) complexed by O/N or S functional groups in humic acids while accounting for time-dependent structural rearrangement. Geochem. Cosmochim. Acta 154, 151–167.

Jiang, T., Kaal, J., Liang, J., Zhang, Y., Wei, S., Wang, D., Green, N.W., 2017. Composition of dissolved organic matter (DOM) from periodically submerged soils in the three gorges reservoir areas as determined by elemental and optical analysis, infrared spectroscopy, pyrolysis-GC-MS and thermally assisted hydrolysis and methylation. Sci. Total Environ. 603–604, 461–471.

Jiang, T., Bravo, A.G., Skyllberg, U., Björn, E., Wang, D., Yan, H., Green, N.W., 2018a. Influence of dissolved organic matter (DOM) characteristics on dissolved mercury (Hg) species composition in sediment porewater of lakes from Southwest China. Water Res. 146, 146–158.

Jiang, T., Chen, X., Wang, D., Liang, J., Bai, W., Zhang, C., Wang, Q.L., Wei, S.Q., 2018c. Dynamics of dissolved organic matter (DOM) in a typical inland lake of the three gorges reservoir area: fluorescent properties and their implications for dissolved mercury species. J. Environ. Manag. 206, 418–429.

Jiang, T., Kaal, J., Liang, J., Liu, J., Zhang, Y.L., Wang, D.Y., Wei, S.Q., Zhao, Z., 2019. Use of the nitrogen /carbon ratio (N/C) and two end-member sources mixing model to identify the origins of dissolved organic matter from soils in the water-level fluctuation zones of the Three Gorges Reservoir. Environ. Sci. 40 (6), 2647–2656 (in Chinese).

Jiang, T., Wang, D., Meng, B., Chi, J., Laudon, H., Liu, J., 2020b. The concentrations and characteristics of dissolved organic matter in high-latitude lakes determine its ambient reducing capacity. Water Res. 169, 115217.

Jiang, T., Wang, D., Wei, S., Yan, J., Liang, J., Chen, X., Liu, J., Wang, Q.L., Lu, S., Gao, J., Li, L.L., Guo, N., Zhao, Z., 2018b. Influences of the alternation of wet-dry periods on the

variability of chromophoric dissolved organic matter in the water level fluctuation zone of the Three Gorges Reservoir area, China. Sci. Total Environ. 636, 249–259.

Kaal, J., Cortizas, A.M., Rydberg, J., Bigler, C., 2015. Seasonal changes in molecular composition of organic matter in lake sediment trap materials from Nylandssjön, Sweden. Org. Geochem. 83–84, 253–262.

Kalbitz, K., Schmerwitz, J., Schwesig, D., Matzner, E., 2003a. Biodegradation of soil-derived dissolved organic matter as related to its properties. Geoderma 113, 273–291.

Kalbitz, K., Schwesig, D., Schmerwitz, J., Kaiser, K., Haumaier, L., Glaser, B., Ellerbrock, R., Leinweber, P., 2003b. Changes in properties of soil-derived dissolved organic matter induced by biodegradation. Soil Biol. Biochem. 35, 1129–1142.

Kamjunke, N., Oosterwoud, M.R., Herzsprung, P., Tittel, J., 2016. Bacterial production and their role in the removal of dissolved organic matter from tributaries of drinking water reservoirs. Sci. Total Environ. 548–549, 51–59.

Kellerman, A.M., Guillemette, F., Podgorski, D.C., Aiken, G.R., Butler, K.D., Spencer, R.G.M., 2018. Unifying concepts linking dissolved organic matter composition to persistence in aquatic ecosystems. Environ. Sci. Technol. 52, 2538–2548.

Kim, S., Kaplan, L.A., Hatcher, P.G., 2006. Biodegradable dissolved organic matter in a temperate and a tropical stream determined from ultra-high resolution mass spectrometry, Limnol. Oceanogr. 51 (2), 1054–1063.

Koehler, B., Von Wachenfeldt, E., Kothawala, D., Tranvik, L.J., 2012. Reactivity continuum of dissolved organic carbon decomposition in lake water. J. Geophys. Res. 117, 1–14.

Kothawala, D.N., Von Wachenfeldt, E., Koehler, B., Tranvik, L.J., 2012. Selective loss and preservation of lake water dissolved organic matter fluorescence during long-term dark incubations. Sci. Total Environ. 433, 238–246.

Kristensen, E., Ahmed, S.I., Devol, A.H., 1995. Aerobic and anaerobic decomposition of organic matter in marine sediment: which is fastest? Limnol. Oceanogr. 40, 1430–1437.

LaRowe, D.E., Van Cappellen, P., 2011. Degradation of natural organic matter: a thermodynamic analysis. Geochem. Cosmochim. Acta 75 (8), 2030–2042.

Lee, C., 1992. Controls on organic carbon preservation: the use of stratified water bodies to compare intrinsic rates of decomposition in oxic and anoxic systems. Geochim. Cosmochim. Acta 56, 3323–3335.

Lee, M., Osburn, C.L., Shin, K., Hur, J., 2018. New insight into the applicability of spectroscopic indices for dissolved organic matter (DOM) source discrimination in aquatic systems affected by biogeochemical processes. Water Res. 147, 164–176.

Liu, H., Wu, Y., Ai, Z., Zhang, J., Zhang, C., Xue, S., 2019a. Effects of the interaction between temperature and revegetation on the microbial degradation of soil dissolved organic matter (DOM)-a DOM incubation experiment. Geoderma 337 (26), 812–824.

Liu, J., Jiang, T., Kothawala, D.N., Wang, Q., Zhao, Z., Wang, D., Mu, Z., Zhang, J.Z., 2019b. Rice-paddy field acts as a buffer system to decrease the terrestrial characteristics of dissolved organic matter exported from a typical small agricultural watershed in the Three Gorges Reservoir Area, China. Environ. Sci. Pollut. Res. 26, 23873–23885.

Mao, R., Chen, H., Li, S., 2017. Phosphorus availability as a primary control of dissolved organic carbon biodegradation in the tributaries of the Yangtze River in the Three Gorges Reservoir region. Sci. Total Environ. 574, 1472–1476.

Marschner, B., Kalbitz, K., 2003. Controls of bioavailability and biodegradability of dissolved organic matter in soils. Geoderma 113, 211–235.

Middelburg, J.J., 1989. A simple rate model for organic matter decomposition in marine sediments. Geochim. Cosmochim. Acta 53, 1577–1581.

Moran, M.A., Sheldon, W.M., Zepp, R.G., 2000. Carbon loss and optical property changes during long-term photochemical and biological degradation of estuarine dissolved organic matter. Limnol. Oceanogr. 45, 1254–1264.

Nierop, K.G.J., Buurman, P., 1998. Composition of soil organic matter and its water-soluble fraction under young vegetation on drift sand Central Netherlands. Eur. J. Soil Sci. 49 (4), 605–615.

Noh, S., Kim, J., Hur, J., Hong, Y., Han, S., 2018. Potential contributions of dissolved organic matter to monomethylmercury distributions in temperate reservoirs as revealed by fluorescence spectroscopy. Environ. Sci. Pollut. Res. 25, 6474–6486.

Obernosterer, I., Benner, R., 2004. Competition between biological and photochemical processes in the mineralization of dissolved organic carbon. Limnol. Oceanogr. 49 (1), 117–124.

Pellerin, B.A., Hernes, P.J., Saraceno, J., Spencer, R.G.M., Bergamaschi, B.A., 2010. Microbial degradation of plant leachate alters lignin phenols and trihalomethane precursors. J. Environ. Qual. 39, 946.

Reimers, C.E., Alleau, Y., Bauer, J.E., Delaney, J., Girguis, P.R., Schrader, P.S., Stercher III, H.A., 2013. Redox effects on the microbial degradation of refractory organic matter in marine sediments. Geochem. Cosmochim. Acta 121, 582–598.

Schartup, A.T., Mason, R.P., Balcom, P.H., Hollweg, T.A., Chen, C.Y., 2013. Methylmercury production in estuarine sediments: role of organic matter. Environ. Sci. Technol. 47, 695–700.

Seidel, M., Beck, M., Riedel, T., Waska, H., Suryaputra, I.G.N.A., Schnetger, B., Niggemann, J., Simon, M., Dittmar, T., 2014. Biogeochemistry of dissolved organic matter in an anoxic intertidal creek bank. Geochem. Cosmochim. Acta 140, 418–434.

Shen, Y., Benner, R., 2020. Molecular properties are a primary control on the microbial utilization of dissolved organic matter in the ocean. Limnol. Oceanogr. 65 (5), 1061–1071.

Sleighter, R.L., Cory, R.M., Kaplan, L.A., Abdulla, H.A.N., Hatcher, P.G., 2014. A coupled geochemical and biogeochemical approach to characterize the bioreactivity of dissolved organic matter from a headwater stream. J. Geophys. Res. Biogeosci. 119 (8), 1520–1537.

Solomon, C.T., Jones, S.E., Weidel, B.C., Buffam, I., Fork, M.L., Karlsson, J., Larsen, S., Lennon, J.T., Read, J.S., Sadro, S., Saros, J.E., 2015. Ecosystem consequences of changing inputs of terrestrial dissolved organic matter to lakes: current knowledge and future challenges. Ecosystems 18, 376–389.

Sondergaard, M., Middelboe, M., 1995. A cross-system analysis of labile dissolved organic-carbon. Mar. Ecol. Prog. Ser. 118, 283–294.

Stedmon, C.A., Markager, S., 2005. Tracing the production and degradation of autochthonous fractions of dissolved organic matter by fluorescence analysis. Limnol. Oceanogr. 50, 1415–1426.

Stepanauskas, R., Moran, M.A., Bergamaschi, B.A., Hollibaugh, J.T., 2005. Sources, bioavailability, and photoreactivity of dissolved organic carbon in the Sacramento-San Joaquin River Delta. Biogeochemistry 74, 131–149.

Sulzberger, B., Arey, J.S., 2016. Impacts of polar changes on the UV-induced mineralization of terrigenous dissolved organic matter. Environ. Sci. Technol. 50, 6621–6631.

Sun, M.Y., Aller, R.C., Lee, C., Wakeham, S.G., 2002. Effects of oxygen and redox oscillation on degradation of cell-associated lipids in surficial marine sediments. Geochem. Cosmochim. Acta 66 (11), 2003–2012.

Tranvik, L.J., Downing, J.A., Cotner, J.B., Loiselle, S.A., Striegl, R.G., Ballatore, T.J., Dillon, P., Finlay, K., Fortino, K., Knoll, L.B., Kortelainen, P.L., Kutser, T., Larsen, S., Laurion, I., Leech, D.M., McCallister, S.L., McKnight, D.M., Melack, J.M., Overholt, E., Porter, J.A., Prairie, Y., Renwick, W.H., Roland, F., Sherman, B.S., Schindler, D.W., Sobek, S., Tremblay, A., Vanni, M.J., Verschoor, A.M., Wachenfeldt, E.V., Weyhenmeyer, G.A., 2009. Lakes and reservoirs as regulators of carbon cycling and climate. Limnol. Oceanogr. 54, 2298–2314.

Vachon, D., Prairie, Y.T., Giorgio, P.A., 2017. Modeling allochthonous dissolved organic carbon mineralization under variable hydrologic regimes in boreal lakes. Ecosystems 781–795.

Valle, J., Gonsior, M., Harir, M., Enrich-prast, A., Schmitt-kopplin, P., Bastviken, D., Conrad, R., Hertkorn, N., 2018. Extensive processing of sediment pore water dissolved organic matter during anoxic incubation as observed by high- field mass spectrometry. Water Res. 129, 252–263.

Wagner, S., Jaffé, R., Cawley, K., Dittmar, T., Stubbins, A., 2015. Associations between the molecular and optical properties of dissolved organic matter in the Florida Everglades, a model coastal wetland system. Front. Chem. 3, 66.

Wang, K., Pang, Y., He, C., Li, P., Xiao, S., Sun, Y., Pan, Q., Zhang, Y., Shi, Q., He, D., 2019. Optical and molecular signatures of dissolved organic matter in Xiangxi Bay and mainstream of Three Gorges Reservoir, China: spatial variations and environmental implications. Sci. Total Environ. 657, 1274–1284.

Ward, N.D., Keil, R.G., Medeiros, P.M., Brito, D.C., Cunha, A.C., Dittmar, T., Yager, P.L., Krusche, A.V., Richey, J.E., 2013. Degradation of terrestrially derived macromolecules in the Amazon River. Nat. Geosci. 6 (7), 530–533.

Wickland, K.P., Neff, J.C., Aiken, G.R., 2007. Dissolved organic carbon in Alaskan boreal forest: sources, chemical characteristics, and biodegradability. Ecosystems 10, 1323–1340.

Xu, H.C., Guo, L.D., 2018. Intriguing changes in molecular size and composition of dissolved organic matter induced by microbial degradation and self-assembly. Water Res. 135, 187–194.

Yu, G.H., Wu, M.J., Wei, G.R., Luo, Y.H., Ran, W., Wang, B.R., Zhang, J.C., Shen, Q.R., 2012. Binding of organic ligands with Al(III) in dissolved organic matter from soil: implications for soil organic carbon storage. Environ. Sci. Technol. 46 (11), 6102–6109.

Zheng, J., Xu, Z., Wang, Y., Dong, H., Chen, C., Han, S., 2014. Non-additive effects of mixing different sources of dissolved organic matter on its biodegradation. Soil Biol. Biochem. 78, 160–169.